Establishing epithelial glandular polarity: interlinked roles for ARF6, Rac1, and the matrix microenvironment

Christine L. Monteleon[a], Alanna Sedgwick[a], Alyssa Hartsell[a], Michael Dai[a], Catherine Whittington[b], Sherry Voytik-Harbin[b], and Crislyn D'Souza-Schorey[a]

[a]Department of Biological Sciences, University of Notre Dame, Notre Dame, IN 46556; [b]Weldon School of Biomedical Engineering, Purdue University, West Lafayette, IN 47907

ABSTRACT **Epithelial cysts comprise the structural units of the glandular epithelium. Although glandular inversion in epithelial tumors is thought to be a potential mechanism for the establishment of metastatic disease, little is known about the morphogenic cues and signaling pathways that govern glandular polarity and organization. Using organotypic cultures of Madin-Darby canine kidney cells in reconstituted basement membrane, we show that cellular depletion of the small GTP-binding protein ARF6 promotes the formation of inverted cysts, wherein the apical cell membrane faces the cyst exterior, and the basal domain faces the central lumen, while individual cell polarity is maintained. These cysts are also defective in interactions with laminin at the cyst–matrix interface. This inversion of glandular orientation is accompanied by Rac1 inactivation during early cystogenesis, and temporal activation of Rac1 is sufficient to recover the normal cyst phenotype. In an unnatural collagen I microenvironment, ARF6-depleted, inverted epithelial cysts exhibit some loss of cell polarity, a marked increase in Rho activation and Rac1 inactivation, and striking rearrangement of the surrounding collagen I matrix. These studies demonstrate the importance of ARF6 as a critical determinant of glandular orientation and the matrix environment in dictating structural organization of epithelial cysts.**

Monitoring Editor
Mark H. Ginsberg
University of California, San Diego

Received: Mar 30, 2012
Revised: Sep 26, 2012
Accepted: Oct 1, 2012

INTRODUCTION

The structural organization of glandular tissues and organs is dependent on the proper assembly of the hollow structural units, such as epithelial cysts, that comprise these tissues. An epithelial cyst is a highly organized structure consisting of a spherical monolayer that surrounds a hollow lumen, wherein each cell has its apical surface facing the cyst lumen, the basal surface apposed to the basement membrane, and the lateral membranes in contact with neighboring cells. As such, the establishment of glandular architecture is largely governed by the cell–cell and cell–matrix interactions. Loss of this polarized glandular organization leads to physiological dysfunction and ultimately to a pathological state (Molitoris and Nelson, 1990).

Organotypic three-dimensional cell culture utilizes an extracellular matrix (ECM)-rich environment in which epithelial cells organize into glandular structures representative of those found in vivo (Bissell *et al.*, 2003; Debnath and Brugge, 2005). Madin-Darby canine kidney (MDCK) cysts develop via a precisely regulated process that has been previously described (O'Brien, 2002; Bryant and Mostov, 2008). In brief, the cyst develops from a single, unpolarized cell. The cell interacts with the ECM environment and then coordinates the distribution of polarity complexes to establish an axis of polarity. Concurrent with the latter step, the cytoskeleton and membrane-trafficking systems organize asymmetrically, such that apical components coalesce at the membrane to establish the apical domain. Thus individual cells become asymmetrically polarized. As the cells in the cyst proliferate, the orientation and organization of this asymmetry must be coordinated between neighboring cells. All cells in a

This article was published online ahead of print in MBoC in Press (http://www.molbiolcell.org/cgi/doi/10.1091/mbc.E12-03-0246) on October 10, 2012.

Address correspondence to: Crislyn D'Souza-Schorey (cdsouzas@nd.edu).

Abbreviations used: ECM, extracellular matrix; EGF, epidermal growth factor; FITC, fluorescein isothiocyanate; GFP, green fluorescent protein; MDCK, Madin-Darby canine kidney; PAK, p21 activated kinase; PSC, porcine skin collagen; siRNA, small interfering RNA.

developing cyst are similarly oriented until the expanding cyst structure reaches maturity. This dynamic culture environment allows investigators to precisely examine the molecular mechanisms that regulate the segregation of specific membrane components and their orientation during the development of epithelial cysts.

Despite its importance, little is known about the physiological cues that promote the unique polarized assembly of epithelial cells in a cyst. The mechanisms involved can be directly investigated and better understood by studying signaling pathways and mechanisms that lead to inverted epithelial cysts. Inverted MDCK cysts were first described in suspension cultures (Wang *et al.*, 1990). Suspended cysts have a center core of basement membrane, and the apical membrane faces the free, external surface. Inverted cysts have also been described in collagen I matrices, wherein seeded cells express the dominant-negative form of the GTPase Rac1, thus demonstrating the importance of Rac1 in orienting the apical domain in MDCK cysts (O'Brien *et al.*, 2001). In a related study, it was shown that blocking the ECM receptor β1 integrin inhibited the activation of Rac1 in matrix overlay cultures and resulted in an inverted MDCK cyst (Yu *et al.*, 2005, 2008). The latter study pointed toward the role of the ECM in providing the physical cue required to orient polarized cysts. In support of this contention, in all cyst inversions, whether due to dominant–negative Rac1, blocking of β1-integrin function, or growth in suspension, epithelial cysts are inverted due to a defect in the ability of the cyst to receive or interpret signals from the ECM.

Previous studies in our laboratory have shown that sustained activation of the Ras-like GTP binding protein ARF6 promotes the internalization and accumulation of some growth factor receptors into signaling endosomes, leading to hyperactive signaling and the formation of aberrant cysts with multiple lumens and the survival of matrix-deprived cells (Tushir *et al.*, 2010). These findings led us to investigate the effects of depleting endogenous ARF6 on cyst formation to better understand the role of ARF6 in normal cyst morphogenesis. Using basement membrane cultures of MDCK cysts, we determined that ARF6 plays an integral role in cyst development, as a small interfering RNA (siRNA)-mediated knockdown of ARF6 expression causes a striking inversion of epithelial cysts. We show that ARF6 activity lies upstream of Rac1 activation and endogenous laminin-332 (formerly termed laminin-5) deposition in a pathway that governs cyst orientation in a basement membrane environment. We also demonstrate the importance of the matrix microenvironment in organizing MDCK cysts and establishing glandular phenotype. The findings reported here are particularly significant, given that inversion of glandular domains is a histopathological abnormality in some epithelial cancers and also in genetic diseases, such as autosomal dominant polycystic kidney disease (Wilson *et al.*, 1991; Adams *et al.*, 2002, 2004; Nassar *et al.*, 2004).

RESULTS

Depletion of ARF6 by siRNA induces the inversion of epithelial cyst orientation

To investigate the role of ARF6 in epithelial cyst organization, we created an MDCK cell line that inducibly expresses an siRNA directed against ARF6 under the control of the tet-operon (described in *Materials and Methods*). In the presence of 3 μg/ml of doxycycline, ARF6 expression was severely repressed. Hereafter, this cell line is referred to as MDCK^{ARF6si}.

When seeded in Matrigel, normal mature epithelial cysts have a distinct and continuous apical domain that faces a hollow internal lumen and a basal surface that is in contact with the matrix. In the experiment described in Figure 1, virtually all parental MDCK cysts establish an apical domain oriented toward the center of the cyst and present a single lumen (Figure 1A; 90%, $n = 490$). On depletion of cellular ARF6 at the onset of cyst development, the vast majority of MDCK^{ARF6si} cysts exhibited a gross misorientation of apical and basolateral domains (Figure 1A; 85%, $n = 390$). The most severe phenotype was a complete reversal in domain orientation that resulted in the formation of "inverted cysts." In some of these cysts, only partial inversion was observed, rendering a "scrambled cyst" appearance (Figure 1, A and B). Domain inversion was characterized by the mislocalization of the intense actin staining (signifying the assembly of microvilli at the apical membrane) toward the cortex of the cyst structure rather than facing the lumen, as seen for parental MDCK cysts. The misorientation of the apical domain in MDCK^{ARF6si} cysts was also demonstrated by the distribution of the apical membrane marker gp135, as well as the *cis*-Golgi marker GM130, which maintains a subapical orientation in polarized MDCK cells. In MDCK^{ARF6si} cysts, gp135 and GM130 oriented toward the cyst periphery, in contrast with their localization toward the lumen in parental MDCK cysts. The mislocalization of the apical domain to the cyst periphery was complete with the mutual exclusion of basolateral markers E-cadherin and β1-integrin (Figure 1A). Thus depletion of ARF6 expression in three-dimensional cultures does not disturb the individual cell polarity, but rather the glandular organization is inverted.

We also knocked down ARF6 expression following cyst polarization and lumen initiation (day 5) during cyst morphogenesis. Under these conditions, lumen maturation was unaffected and normal cysts developed (Figure 1C). Thus ARF6 expression is required for orienting membrane domains during the early stages of cyst development.

To rule out that the effects of ARF6 depletion on glandular organization were not restricted to the clonal cell population, we tested an alternate method of siRNA delivery using lentivirus encoding ARF6 siRNA and green fluorescent protein (GFP). This method resulted in a moderate decrease in ARF6 expression (Supplemental Figure S1). Virus-infected cells were allowed to develop into cysts, and transduction was confirmed with the presence of GFP. Cyst inversion, full or scrambled ($n = 138$, 29%), was the predominant phenotype, although not as penetrant as that described above (Figure S2). In addition to inverted cysts, other aberrant phenotypes, such as stunted cysts, filled cysts, and cysts with abnormal lumens, as well as normal cysts, were observed. The wide array of phenotypes observed using the lentiviral system could be due to varied expression levels of the siRNA hairpin in cysts or the timing of the lentiviral-mediated ARF6 knockdown during cyst morphogenesis. In stark contrast, infection of MDCK cells with lentivirus expressing GFP alone generated only normal cysts (0% inverted, $n = 50$, unpublished data).

To confirm that glandular inversion is a result of ARF6 depletion, we expressed wild-type ARF6 with silent mutations in the region targeted by the siRNA in MDCK^{ARF6si} cysts, using a retrovirus expression plasmid that also encodes GFP. While expression of this ARF6 mutant had no effect on the formation of cysts derived from the parental cell line (unpublished data), it was sufficient to rescue the inverted phenotype of MDCK^{ARF6si} cysts (Figure 2A). Viral particles were applied to cultures at 1 d postseeding, allowing the cyst to develop from a single GFP-positive cell. Though some cells in the mature cysts lost GFP expression by the time of fixation, proliferating cells in a developing MDCK cyst can derive assembly cues from existing cell–cell and cell–matrix interactions (O'Brien *et al.*, 2002; Nelson, 2003). Of the cysts positive for the siRNA-resistant ARF6 transcript, 82% of cysts had established the apical pole in the cyst interior, as indicated by the intense actin

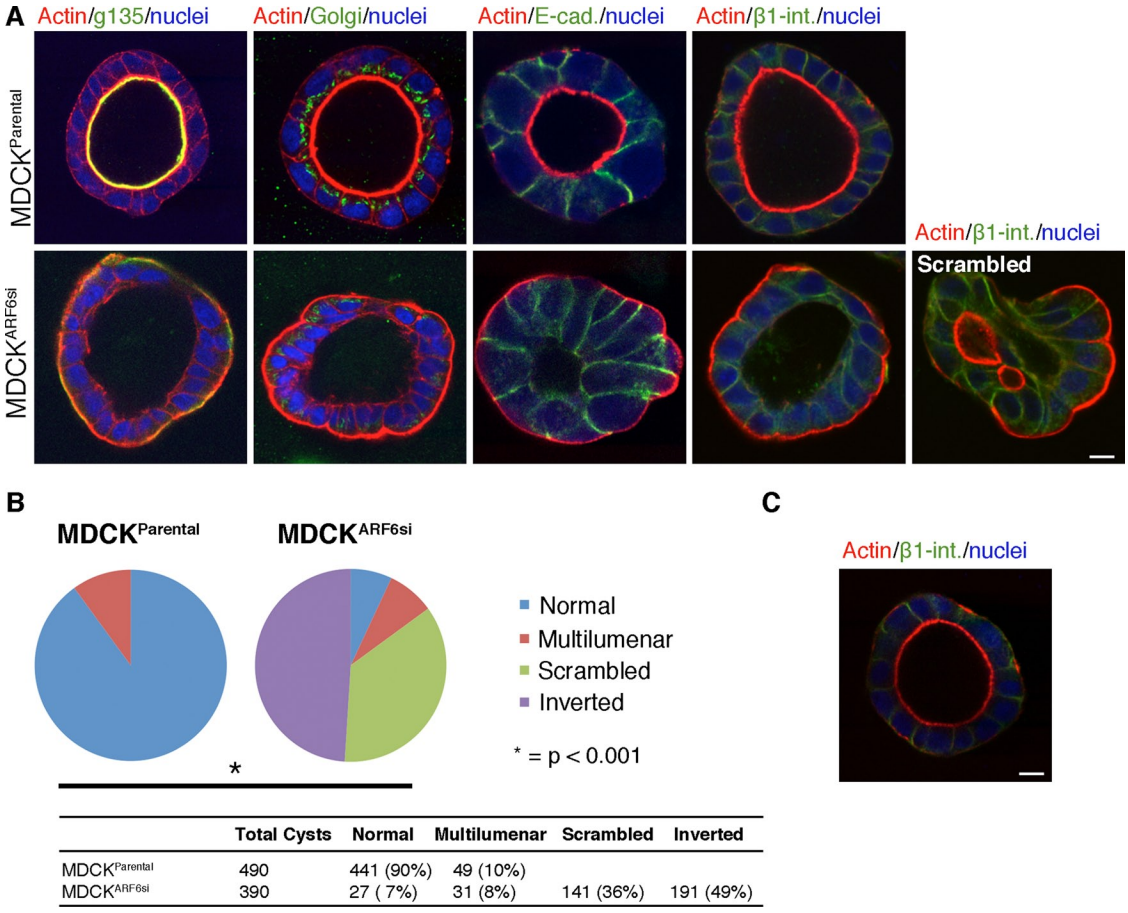

	Total Cysts	Normal	Multilumenar	Scrambled	Inverted
MDCK^{Parental}	490	441 (90%)	49 (10%)		
MDCK^{ARF6si}	390	27 (7%)	31 (8%)	141 (36%)	191 (49%)

FIGURE 1: Depleting ARF6 expression inverts the orientation of MDCK cysts. (A) Parental MDCK and MDCK^{ARF6si} cysts in three-dimensional Matrigel culture were fixed and labeled for nuclei (blue) and actin (red) and either gp135, GM130, β1 integrin, or E-cadherin (green), as indicated. Merged images of single confocal sections through the equatorial plane of the cyst are shown. The localization of the *cis*-Golgi enzyme GM130 and the apical plasma membrane glycoprotein gp135, as well as actin enrichment at the microvilli, demonstrate the assembly of the apical domain at the interior lumen of parental cysts but at the peripheral surface of MDCK^{ARF6si} inverted cysts. β1 integrin and E-cadherin localized to the basolateral domain. MDCK^{ARF6si} cysts were also "scrambled," with portions of the cyst structure displaying an inversion of membrane domains. (B) Parental MDCK and MDCK^{ARF6si} phenotypes were scored by examining cysts systematically through the *z*-axes. Cysts with single, cleared internal lumens were characterized as normal. Inverted and scrambled cysts displayed a complete or partial inversion of domains, respectively, indicated by the assembly of the apical actin band at the periphery of the cyst structure. Cysts with multiple lumens were identified by the presence of several small, apically lined lumens. The distribution of phenotypes as indicated was determined by more than six independent experiments. Significance was assessed by two-tailed paired *z* test from the sum of the experiments. (C) Cyst architecture upon ARF6 knockdown at later stages of cyst development. Cysts were stained for actin (red), E-cadherin (green), and nuclei (blue). Depleting ARF6 at 5 d postseeding had no effect on cyst orientation.

apical banding, and a single lumina was observed in 61% of the cysts (Figure 2B; $n = 91$).

ARF6 knockdown down-regulates critical Rac1 activation in cystogenesis

It has been shown that the expression of a dominant–negative Rac1 mutant during MDCK cystogenesis results in an inverted cyst (O'Brien *et al.*, 2001). ARF6 has been implicated in Rac1 activation during cell migration and invasion, as well as in epithelial tubulogenesis (Santy and Casanova, 2001; Palacios and D'Souza-Schorey, 2003; Tushir and D'Souza-Schorey, 2007, Muralidharan-Chari *et al.*, 2009). We sought to elucidate the activation profile of Rac1 during the formation of parental MDCK and MDCK^{ARF6si} cysts with particular emphasis on the early time points, when the orientation of the pole was being established.

Parental MDCK cysts exhibited a peak in Rac1 activation between days 2 and 4 of cystogenesis. Notably, this spike in Rac1 activation was absent in MDCK^{ARF6si} cultures (Figure 3A). Normal developing cysts grown in Matrigel begin to polarize and form the apical pole shortly after the first doubling, ~2 d postseeding (Figure 3B). These findings corroborate experiments described by Yu *et al.* (2005), showing that Rac1 activation is critical during epithelial morphogenesis. MDCK^{ARF6si} cysts exhibited a small increase to no change in Rho-GTP levels during morphogenesis relative to parental cysts (Figure S3). RhoA activation is higher at seeding and begins to taper as parental MDCK cysts develop.

Activation of Rac1 is sufficient to reorient cyst polarity

We questioned whether stimulating Rac1 downstream of ARF6 depletion could rescue inverted polarity in MDCK^{ARF6si} cysts. We

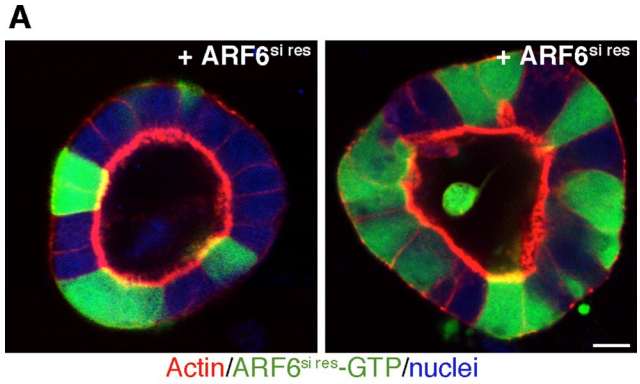

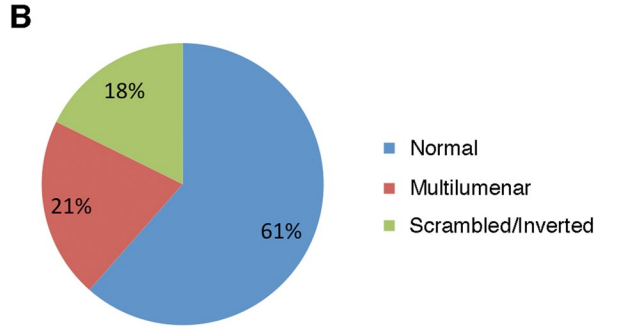

	Total	Normal	Multi	Scrambled/ Inverted
MDCK^{ARF6si}+ ARF6 siRNA resistant transcript	91	56 (21%)	19 (21%)	16(18%)

FIGURE 2: The expression of exogenous ARF6$^{si\text{-}res}$ rescues the inversion of MDCK^{ARF6si} cysts. (A) MDCK^{ARF6si} cells were infected 1 d postseeding with retrovirus encoding a wild-type siRNA-resistant ARF6 construct and GFP. Cysts were allowed to develop and were fixed and processed to visualize actin (red) and nuclei (blue). Although there is a loss of GFP expression in some cells of the mature cyst, cysts were developed from a single infected cell. Exogenous ARF6 expression restores normal glandular orientation. (B) Quantification of the "rescued" phenotypes. On infection with retrovirus encoding ARF6$^{si\text{-}res}$, 61% of infected cysts displayed a single lumen (n = 91), whereas 21% displayed multiple, smaller, apically lined lumens.

assessed whether treatment of MDCK^{ARF6si} cells with epidermal growth factor (EGF), a Rac1 activator and commercially available as CN02, would increase Rac1-GTP levels. As described in *Materials and Methods*, EGF is standardized in CN02 by measurement in units. We showed that CN02 (EGF) is sufficient to up-regulate Rac1 activation independent of the expression of ARF6 (Figure 4A). Moreover, CN02 treatment of MDCK^{ARF6si} cyst cultures resulted in normal cysts, compared with cultures without Rac1 stimulation, and this recovery to normal phenotype was time-dependent (Figure 4B). Recovery was most efficacious if CN02 was applied to developing cysts between 1 and 2 d after cells were seeded, with 66% of the cysts in these cultures displaying a normal phenotype (n = 150) in comparison with only 20% of MDCK^{ARF6si} cysts without CN02/EGF (n = 150; Figure 4C).

For confirmation Rac1-GTP–induced recovery of the MDCK^{ARF6si} inverted-cyst phenotype, constitutively active Rac1 (Rac1(G12V)) was introduced to MDCK^{ARF6si} cyst cultures using retroviral transduction, with GFP as a marker for cell infection. Introduction of Rac1(G12V) did not alter the phenotype of the parental MDCK cysts, and these cysts were indistinguishable from uninfected cysts (Figure 4D; n = 58). The MDCK^{ARF6si} cysts expressing activated Rac1 were largely recovered to a normal cyst phenotype (Figure 4, D and E; 90% normal, n = 158). The effects of EGF and Rac1(G12V), as described above, coupled with the altered Rac1 activation during cystogenesis in MDCK^{ARF6si} cysts, make a compelling case for ARF6-regulated modulation of Rac1 activation during cystogenesis.

Depleting ARF6 disrupts the dynamics of the cyst–matrix interface

The distribution of molecules at the cell–matrix interface has been demonstrated to play a critical role in the organization of epithelial glandular units (Jiang *et al.*, 1999; Yu *et al.*, 2005). Both laminins and β1 integrins have been implicated in establishing the orientation of MDCK cysts. In normal cysts, β1 integrin is targeted to the basolateral membrane of cells, where it interacts with matrix components and organizes the actin cytoskeleton during cyst development (Yamada and Geiger, 1997). As indicated earlier, in MDCK^{ARF6si} inverted cysts, β1 integrin was still localized to the basolateral plasma membrane (also shown in Figure 5A). Thus the integrin receptor is still targeted to the plasma membrane as in parental cells, even when the basolateral membrane is not exposed to the matrix.

To further characterize the cyst–matrix interface, we investigated the assembly of laminins at the cyst periphery. To initiate these investigations, we first analyzed the distribution of endogenous laminin, laminin-332. Laminin-332 is produced and secreted by MDCK cysts and has no subunits in common with laminin-111, the main component of Matrigel. The laminin-332 signal can therefore be used to identify secreted matrix proteins at the basement membrane–cell interface. In normal cysts, laminin-332 was assembled in a uniform, supportive structure around the cyst periphery (Figure 5B). However, the organization of laminin-332 was severely perturbed in MDCK^{ARF6si} inverted cysts. The distinctive supporting structure of laminin-332 seen in parental MDCK cysts was not observed at the periphery of the inverted MDCK^{ARF6si} cysts (Figure 5B). In scrambled MDCK^{ARF6si} cysts, there was a deposition of laminin-332 in regions of the cyst in which the basolateral domain was oriented toward the periphery of the cyst. It has been described that occupied integrins are likely the trigger for the secretion of cellular laminins (Rodriguez-Boulan and Salas, 1989), and the depletion of ARF6 does not appear to interfere with this signal where it is still functional.

Next we attempted to visualize the distribution of the reconstituted basement membrane around parental MDCK and MDCK^{ARF6si} cysts using a laminin-111 antibody. In parental MDCK cysts, the exogenous laminin-111 behaved similarly to the endogenous laminin-332 and was tightly assembled at the periphery of the cyst structure, providing support to the expanding epithelial structure (Figure 5C). However, in MDCK^{ARF6si} cysts, the exogenous laminin-111 was not in contact with the inverted domains of MDCK^{ARF6si} cysts. As seen in Figure 5C, where the cyst displays an inversion of domains, the cells are no longer in contact with matrix. These scrambled cysts appear to be evading the confines of the exogenous matrix, assembling their apical domains at the free surface, clear of laminin-111. We propose that the absence of matrix as a polarizing cue likely contributes to the inversion of polarity.

Because we established that Rac1 stimulation could rescue a normal cyst phenotype for MDCK^{ARF6si} cysts, we sought to determine whether Rac1 activation by CN02 /EGF treatment could also restore the supportive laminin-111 microenvironment. Where CN02

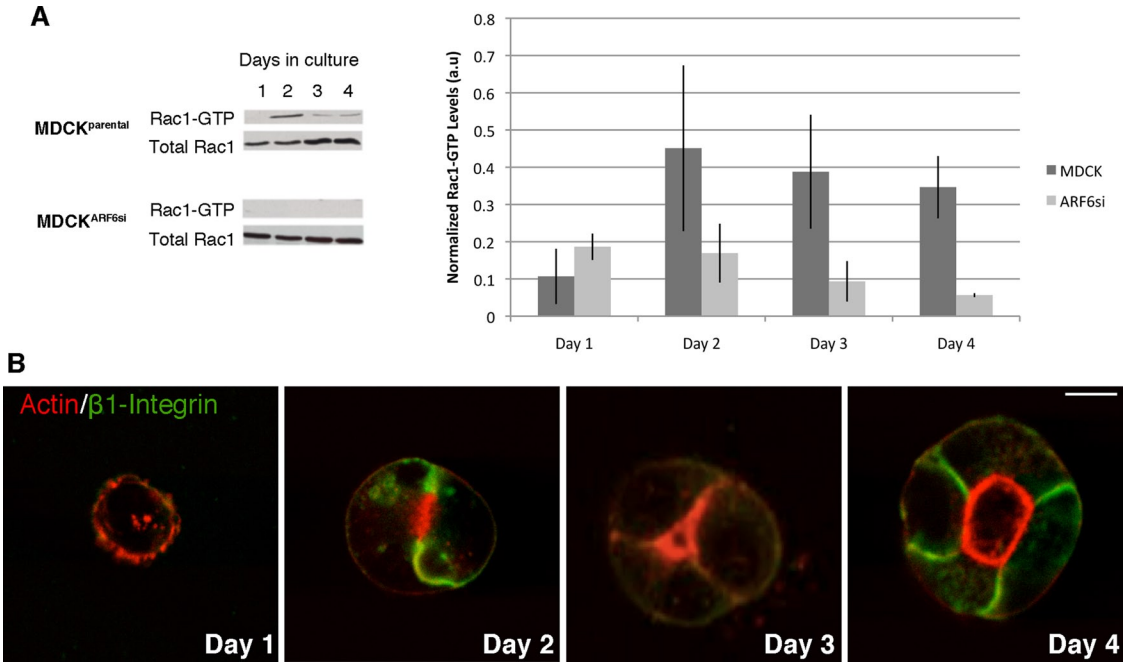

FIGURE 3: ARF6-mediated activation of Rac1 is required for normal cyst assembly. (A) Rac1-GTP levels were assessed by the PAK-GST pull-down assay through consecutive days of cystogenesis in parental MDCK and MDCK^{ARF6si} cysts. Cyst lysates were also examined for total Rac1 expression by Western blotting procedures. The increase in Rac1 activation observed early in parental MDCK cysts was absent in MDCK^{ARF6si} cysts. (B) Equatorial planes of cysts representative of early cystogenesis, from day 1 through day 4 are shown. Cysts were labeled for actin (red) and β1 integrin (green). Cells begin to polarize in Matrigel on day 1, and distinct polarization between apical and basolateral markers is seen by day 2.

treatment recovered a normal phenotype for MDCK^{ARF6si} cysts, the exogenous laminin-staining pattern characteristic of normal cysts was also invariably restored (Figure 5D). Where the CN02 recovery was not completely penetrant and the MDCK^{ARF6si} cysts were still inverted, laminin assembly continued to be perturbed (Figure 5D). Similarly, the CN02 treatment also recovered the deposition of endogenous laminin-332 in cysts in which the phenotype was recovered (Figure 5E). These studies support interlinked roles for ARF6, Rac1, and laminin assembly in regulation of the orientation of epithelial cysts.

Depletion of ARF6 in a collagen I microenvironment causes a loss in cell polarity and matrix rearrangements

Inverted-cyst phenotypes as they relate to Rac1 inhibition or the blocking of β1-integrin function were originally described in collagen I microenvironments (O'Brien *et al.*, 2001; Yu *et al.*, 2005, 2008). These studies demonstrated that the orientation of MDCK cysts depends on the interaction of cells with the ECM. In this study, we also examined whether the inversion of MDCK^{ARF6si} cysts was matrix-dependent by monitoring cyst development in porcine skin collagen (PSC), a reconstituted collagen I matrix. This microenvironment also allows for direct examination of the physical properties of the matrix (Kreger *et al.*, 2010).

In PSC matrix, parental MDCK cysts developed normally, presenting a distinct and continuous apical domain that faced a clear, internal lumen, and a basal surface that was in contact with the matrix. Similar to the MDCK^{ARF6si} phenotype in a basement membrane environment, when cultured in PSC matrix, MDCK^{ARF6si} cysts displayed an intense apical actin banding at the periphery of the cyst structures (Figure 6A). Thus ARF6 plays a crucial role in cyst organization irrespective of the matrix microenvironment.

We investigated the cyst–collagen interface using confocal reflection microscopy combined with fluorescence confocal microcopy. In the parental MDCK cysts, the collagen fibrils were in contact with the basal surface of the cyst, supporting the glandular structure. When MDCK^{ARF6si} cysts were grown in collagen I, there was significant reorganization of the matrix relative to the parental MDCK cysts, with radial realignment of collagen bundles around the MDCK^{ARF6si} cysts (Figure 6B). The matrix surrounding MDCK^{ARF6si} cysts appeared more dense and the collagen fibrils more perpendicular to the surface of the cyst relative to parental cells.

The linearization of collagen fibrils by MDCK^{ARF6si} cysts led us to further investigate the localization of specific apical and basolateral proteins in PSC-grown cysts. There was a peripheral localization of gp135 corresponding to the intense apical actin banding at the periphery of PSC-grown MDCK^{ARF6si} cysts (Figure 6C). However, the PSC-grown MDCK^{ARF6si} cysts were not as distinctly polar as the MDCK^{ARF6si} cysts grown in basement membrane. For instance, the signal for β1 integrin was distributed throughout the basolateral domains of cells in PSC-grown parental MDCK cysts. However, in stark contrast with MDCK^{ARF6si} cyst developed in basement membrane culture, there was a concentration of labeling at the periphery of PSC-grown MDCK^{ARF6si} cysts that colocalized with the strong actin banding at the cortex (Figure 6C). The selective redistribution of β1 integrin at the cyst periphery in PSC-grown MDCK^{ARF6si} cysts correlates well with the ability to interact with and linearize surrounding collagen fibrils. Additionally, as shown in Figure 6C, the activation of the β1 integrin at the periphery of the PSC-grown MDCK^{ARF6si} cysts allows for the deposition of endogenous laminins at the cortex of the cyst, a signal absent in inverted cysts grown in Matrigel.

The matrix linearization and realignment seen in MDCK^{ARF6si} cysts grown in the PSC environment suggests generation of

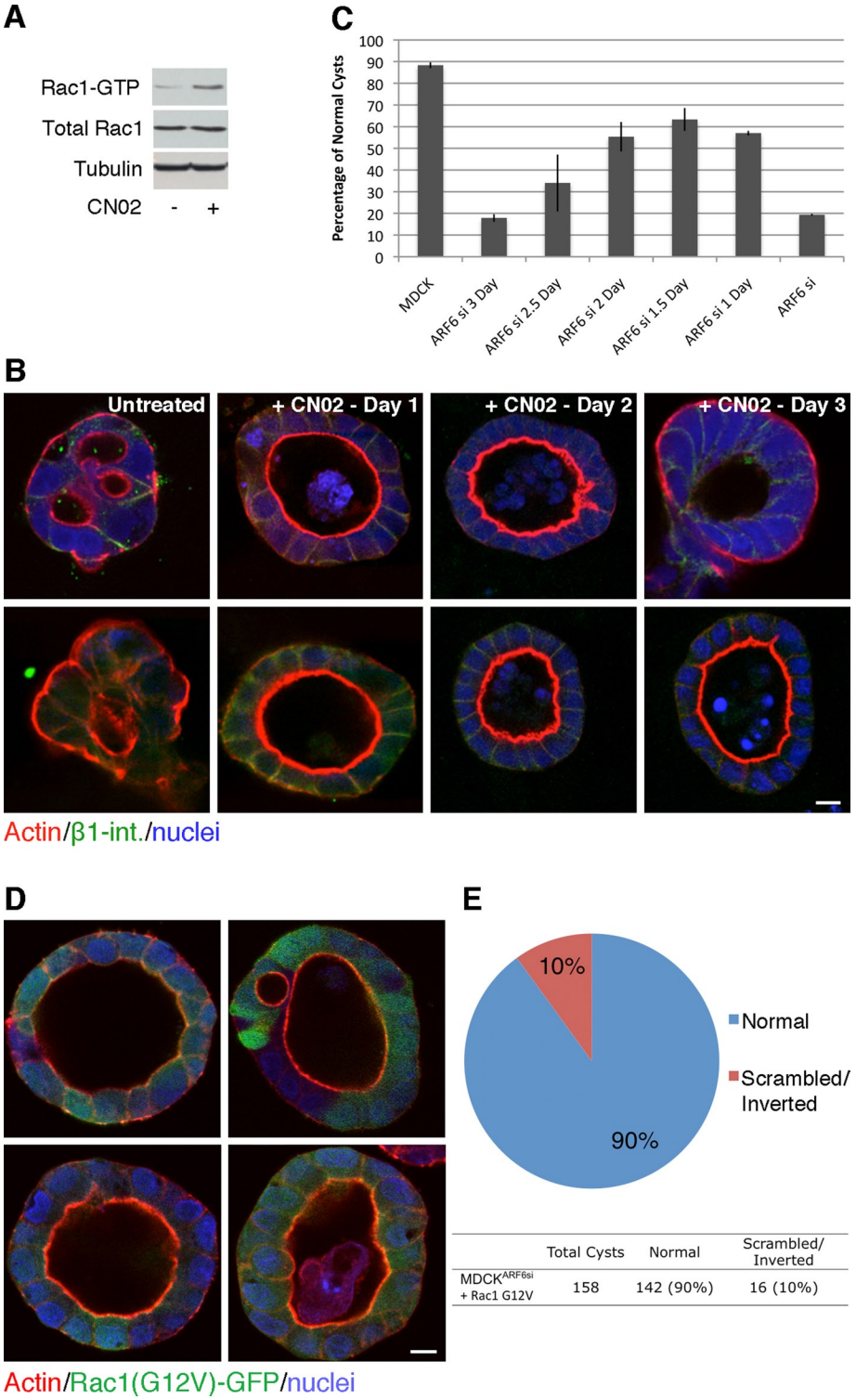

FIGURE 4: Rac1 activation restores normal glandular orientation of MDCK^{ARF6si} cysts. (A) Rac1-GTP in MDCK^{ARF6si} cells with or without CN02/EGF treatment were assessed by PAK-GST pull-down assay. CN02 increases Rac1-GTP levels in MDCK^{ARF6si} cells. Cell lysates were also examined for total Rac1 expression by Western blotting procedures. (B) Representative confocal images of MDCK^{ARF6si} cysts without and with CN02 treatment. Fully developed cysts were stained for actin (red), β1 integrin (green), and nuclei (blue). CN02-treated MDCK^{ARF6si} cysts show a normal phenotype, comparable with parental cysts. (C) CN02 treatment restores a normal phenotype in MDCK^{ARF6si} cysts in a time-dependent manner. CN02 treatment of MDCK^{ARF6si} cysts between days 1 and 2 of MDCK^{ARF6si} cyst development was the most effective at restoring normal phenotype. In each case, more than 50 cysts were scored. The graph represents the mean ± SEM of three separate experiments. (D) Expression of Rac1(G12V) rescues MDCK^{ARF6si} inverted-cyst phenotype. MDCK and MDCK^{ARF6si} cysts were infected with retrovirus encoding Rac1(G12V) and GFP at 1 d postseeding. Parental MDCK cysts were largely unaffected by expression of Rac1(G12V); however, Rac1(G12V) expression was sufficient to restore a normal cyst phenotype in MDCK^{ARF6si} cysts. (E) Quantification of the phenotypes displayed by MDCK^{ARF6si} cysts infected with Rac1(G12V) retrovirus. On infection, 90% of the MDCK^{ARF6si} cysts were rescued to form internal apical domains (n = 158).

contractile force at the cyst–matrix interface that may cause localized stiffening of the microenvironment. It has been previously demonstrated that when matrix rigidity is increased, this stiffness correlates with RhoA signaling in three-dimensional mammary epithelial cell colonies (Paszek *et al.*, 2005). This enhanced stiffness is accompanied by alterations in cell polarity, as well as lumen formation (Paszek *et al.*, 2005). Additionally, inverted collagen-grown MDCK cysts were associated with increased RhoA activation (Yu *et al.*, 2008). Corroborating these findings, we found that MDCK^{ARF6si} in collagen I exhibited a marked enhancement in RhoA-GTP levels and a decrease in Rac1-GTP (Figure S4). We examined whether matrix realignment in MDCK^{ARF6si} cysts was coupled to RhoA signaling. Downstream RhoA signaling was inhibited by the application of Y27632, a selective inhibitor of ROCK (Rho-associated protein kinase). When applied to MDCK^{ARF6si} cysts in PSC matrix, treatment with Y27632 restored a normal cyst phenotype, as well as normal arrangement of collagen fibrils (Figure 7). We also treated PSC-grown MDCK^{ARF6si} cysts with CN02, and the stimulation of Rac1 was capable of restoring cysts and collagen fibrils to the normal phenotype (Figure 7). However, ROCK inhibition had no effect on the inverted-cyst phenotype when applied to MDCK^{ARF6si} cysts in basement membrane cultures (Figure S5). As described earlier, in the basement membrane Matrigel environment, MDCK^{ARF6si} cysts exhibited only a weak activation of RhoA. It is plausible that the β1 integrin at the cyst periphery in PSC-grown cysts can engage the collagen I matrix, leading to RhoA activation and subsequent ROCK activity. Collectively these observations underscore the decisive influence of the cyst microenvironment on cellular signaling and glandular architecture.

DISCUSSION

The establishment of multicellular epithelial glandular units, such as cysts and tubules,

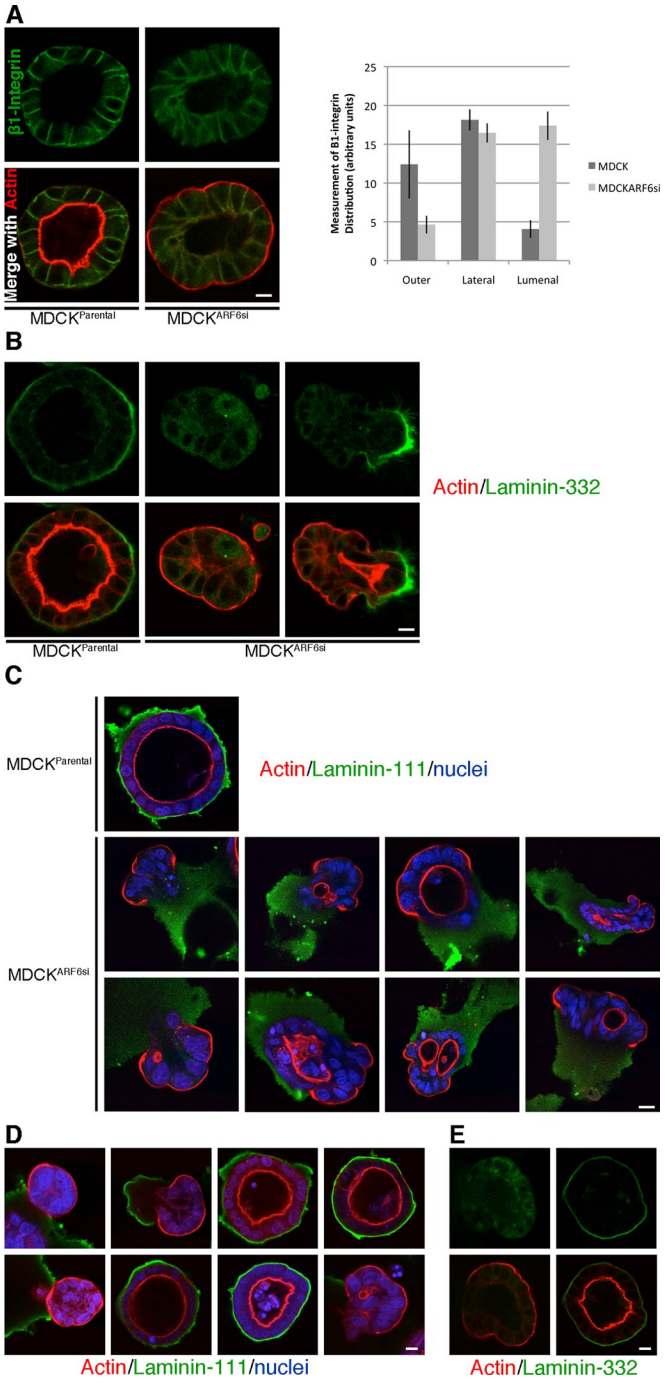

FIGURE 5: The inversion of MDCK^{ARF6si} cysts disrupts the localization of laminins and β1 integrin. (A) The distribution of β1 integrin in MDCK and MDCK^{ARF6si} cysts. Cysts were fixed and labeled for actin (red) and β1 integrin (green). In both MDCK and MDCK^{ARF6si} cysts, β1 integrin is appropriately targeted to the plasma membrane. However, in the MDCK^{ARF6si} inverted cysts, the basolateral domain is not in contact with the matrix, and it is likely that β1 integrin is not occupied by the ECM. For quantifying β1-integrin labeling, the outer, luminal, and lateral domains of 25 cells on representative images were quantified, and the signal intensity was measured using the Image J program. The mean signal intensity was determined, and the averages of these intensities was graphed ± SD. β1 integrin was predominantly at the outer and lateral surfaces of parental cysts and at the lateral and luminal surfaces of inverted MDCK^{ARF6si} cysts. (B) The distribution of laminin-332 in MDCK and MDCK^{ARF6si} cysts. Cysts were fixed and labeled for actin (red) and laminin-332 (green). In parental cysts, laminin-332 is assembled at the cyst–matrix interface; in inverted MDCK^{ARF6si} cysts, laminin-332 remains unassembled; and in scrambled MDCK^{ARF6si} cysts, laminin-332 is deposited at sites at which the basolateral domain is in contact with the matrix. (C) Distribution of laminin-111 in MDCK and MDCK^{ARF6si} cysts. Cysts were fixed and stained for laminin-111 (green), gp135 (red), and nuclei (blue). The exogenous laminin provides support around the parental cyst. In the MDCK^{ARF6si} cultures, the inverted apical domains appear to be evading the confines of the exogenous matrix and are assembled at the free surface, clear of supportive laminin-111. (D) Activation of Rac1 is sufficient to rescue laminin-111 organization around the cyst. Representative images of EGF/CN02-treated cysts labeled for actin (red), laminin-111 (green), and nuclei (blue) are shown. Treatment with CN02 recovered normal cyst phenotypes in MDCK^{ARF6si} cysts and the supportive assembly of laminin-111. The recovery was most effective when MDCK^{ARF6si} cysts were treated with CN02 at day 2 of cyst development. When the recovery of the MDCK^{ARF6si} phenotypes was not completely penetrant, the exogenous laminin continued to be disassociated from the apical domains of the scrambled or inverted cysts. (E) Activation of Rac1 is sufficient to rescue laminin-332 deposition in support of the cyst. MDCK^{ARF6si} cysts were labeled for actin (red) and laminin-332 (green). Treatment with CN02 recovered normal cyst phenotypes in MDCK^{ARF6si} cysts, as well as the deposition of laminin-332 at the cyst–matrix interface.

allows tissues that comprise these structures to function in a capacity that would not be possible without this structural organization. Much remains to be understood about how these multicellular structures assemble. As elucidated here, three-dimensional culture provides a tractable system to better understand the critical processes and environmental cues necessary for cyst morphogenesis. We have shown that MDCK cysts depleted of endogenous ARF6 form grossly misoriented "inverted" cysts. The apical domain of MDCK^{ARF6si} cells aberrantly displayed at the periphery of inverted cysts does not interact with the matrix microenvironment, as do normal epithelial cysts. Moreover, the nature of the microenvironment significantly influences glandular phenotype. While MDCK^{ARF6si} cysts grown in basement membrane are incapable of associating with laminin-111 to support the growing cyst, in an interstitial collagen I microenvironment, MDCK^{ARF6si} cysts engage in fibril attachments via integrin receptors to promote fibrillar linearization reminiscent of matrix stiffening in disease states.

The MDCK^{ARF6si} cysts in reconstituted basement membrane with inverted apical domains dissociated from the matrix are reminiscent of suspension-grown cysts, which also exhibit inverted domains due to lack of interaction with the matrix. This inability of MDCK^{ARF6si} cysts to engage the reconstituted basement membrane is also likely responsible for their inability to activate Rac1. It has been shown previously that the matrix receptor β1 integrin is responsible for the transient activation of Rac1 upon morphogenic initiation in response to ECM (Yu *et al.*, 2005). In this study, the transient activation of Rac1 coincided with the delivery and assembly of endogenous ECM proteins at the cortex of the parental MDCK cysts. Our working model (Figure 8) suggests that Rac1 and receptor activity resultant from basement membrane deposition act in a positive-feedback mechanism downstream of ARF6 to promote proper polarization and orientation of domains during cyst formation. An earlier study assessing the effects of dominant-negative Rac1 suggested that Rac1 is required for the assembly of endogenous laminins in developing epithelial cysts (O'Brien *et al.*, 2001; Yu *et al.*, 2005). Our data support this contention and demonstrate that the activation of Rac1 in inverted cysts restores association with laminins and the normal cyst phenotype. According to our working model, the assembly of

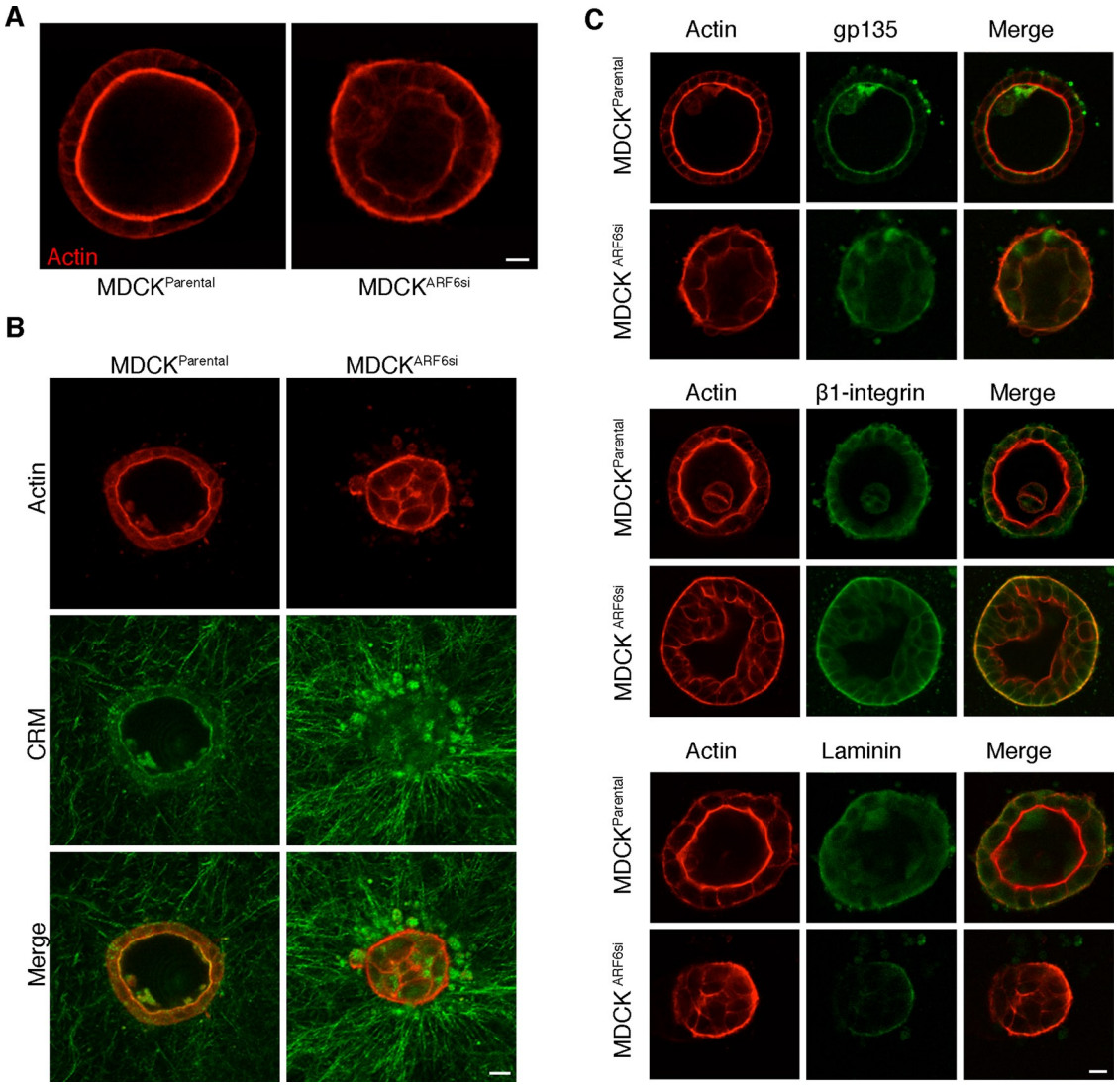

FIGURE 6: Depletion of ARF6 in collagen I matrix induces loss of cell polarity and matrix rearrangements. (A) MDCK and MDCK^{ARF6si} cysts in PSC matrix were fixed and stained for actin. PSC-grown MDCK cysts displayed single lumens, whereas MDCK^{ARF6si} cysts exhibited intense apical actin banding at the cyst periphery. (B) PSC cultures of MDCK and MDCK^{ARF6si} cysts stained for actin (red) and processed for confocal reflection microscopy (CRM) to allow visualization of collagen I fibrils (green). In parental MDCK cysts, the collagen fibrils closely appose the basal surface of the cyst, supporting the glandular structure. In the MDCK^{ARF6si} cyst cultures, radial and linearized collagen bundles were observed. (C) PSC cultures of MDCK and MDCK^{ARF6si} cysts were stained for actin (red) and gp135, β1 integrin, or endogenous laminin, as indicated. gp135 localizes predominantly to the periphery of the cyst. β1 integrin is at the basolateral membranes of cells in the parental MDCK cysts. In the MDCK^{ARF6si} cysts, a high concentration of β1-integrin signal strongly colocalized with strong actin banding at the cyst–matrix interface of MDCK^{ARF6si} cysts, indicating that there is a selective redistribution of β1 integrin to the periphery of PSC-grown MDCK^{ARF6si} cysts and that polarity is perturbed. Deposition of endogenous laminins at the cyst–matrix interface is detected both with and without ARF6 depletion.

basement membrane proteins activates an increasing number of ECM receptors in a time-dependent manner. In MDCK^{ARF6si} cysts, the initial β1-integrin signal of the seeder cells is preempted, resulting in no activation of Rac1, and therefore no positive-feedback loop between the deposition of endogenous basement membrane components and the activation of Rac1 that is required for cysts to develop an internal apical pole. As a result, MDCK^{ARF6si} cysts develop without matrix-derived cues and resemble those grown in suspension.

It is well understood that matrix composition can influence the cellular and molecular response to microenvironments. For example, cyst development in collagen I is markedly different in comparison with growth in Matrigel, with slower rates of proliferation, polarization, and cystogenesis (Martin-Belmonte and Mostov, 2008). We have found that the application of ROCK inhibitor is sufficient in recovery of inverted MDCK^{ARF6si} cysts, but only when cysts are grown in collagen I. ROCK-inhibition treatment has no effect on MDCK^{ARF6si} cysts grown in Matrigel. When MDCK^{ARF6si} cysts are grown in collagen I, there is a selective redistribution of β1 integrin to the periphery associated with a striking remodeling of the collagen I microenvironment that suggests localized matrix stiffening. It is likely that the ARF6 depletion–related β1-integrin clustering and matrix stiffening

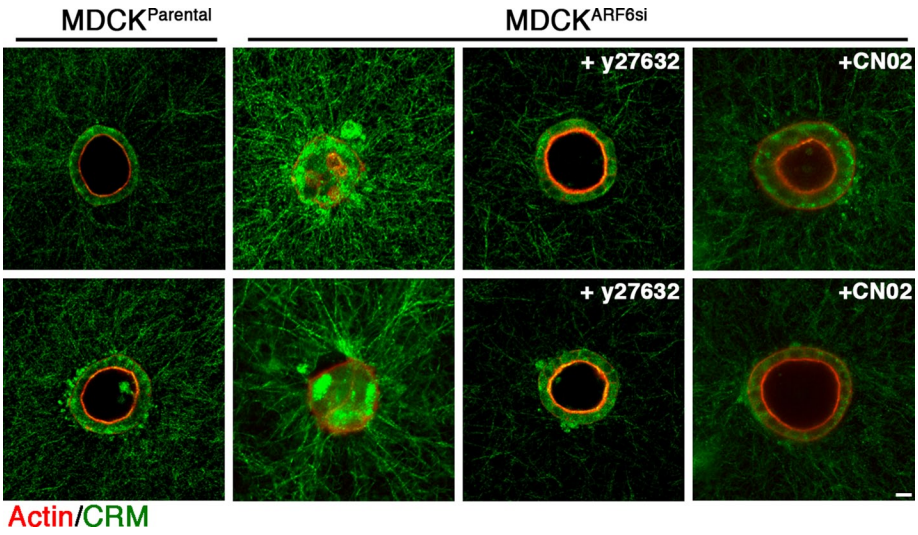

FIGURE 7: Inhibition of ROCK, or activation of Rac1, in PSC-grown MDCK^{ARF6si} cysts is sufficient to recover cyst orientation and normal arrangement of collagen fibrils. PSC cultures of MDCK cysts or MDCK^{ARF6si} cysts treated with either Y27632 or CN02 were stained for actin (red) and processed for confocal reflection microscopy (CRM; green). Treatment of MDCK^{ARF6si} cysts with Y27632 or CN02 restored normal cyst phenotypes and assembly of collagen I fibrils was similar to that seen in parental cyst cultures.

leads to RhoA activation, and subsequently ROCK activity, through previously delineated pathways involving focal adhesion kinase (Paszek *et al.*, 2005; Hebner *et al.*, 2008; Levental *et al.*, 2009). This pathway is responsive to treatment with Y27632. The β1 integrin of MDCK^{ARF6si} cysts in reconstituted basement membrane does not interact with, and as such would not contract, the matrix. Instead, we propose, as others have (Yu *et al.*, 2008; Sanz-Moreno *et al.*, 2008), that there may be a yet to be fully elucidated negative-feedback loop between Rac1 and RhoA, wherein an inability to properly activate Rac1 up-regulates the activation of RhoA by default. Any slight activation of RhoA in MDCK^{ARF6si} cysts in this microenvironment may be related to the suppressed Rac1 activation, rather than through stimulation by canonical signaling. This explains why blocking ROCK does not have the same restorative effect in Matrigel as it does in collagen I. These findings showcase the involvement of the microenvironment in dictating the cellular pathways that regulate epithelial architecture.

Studying the molecular basis for inverted cysts is of high clinical relevance, as cysts with this phenotype are highly reminiscent of histological patterns used to classify a number of diseases. For example, the inversion of domains has been detected in cancers such as malignant mesothelioma (Adams *et al.*, 2002). Notably, this phenotype was prominent particularly at or around blood vessels, which led Adams *et al.* to speculate that exposure of apical membrane components to the vasculature might aid in the formation of metastases (Adams *et al.*, 2002). Inversion of domains has also been detected in invasive ductal carcinoma tumors of the breast, in which there is an observable reversal of glandular polarity in the lymphovascular space (Adams *et al.*, 2004). Here again, given that glandular inversion allows for direct interaction between apical domain–type molecules at the periphery and lymphovascular endothelium, it is hypothesized that a reversal of domains is a mechanism for the establishment of

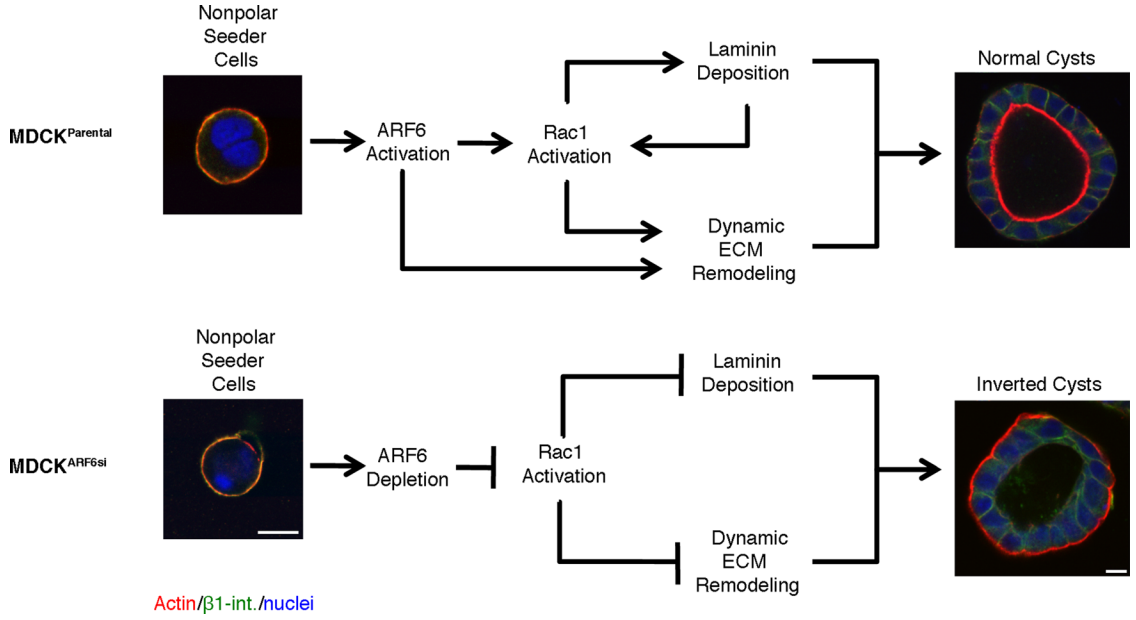

FIGURE 8: Working model for ARF6, Rac1, and basement membrane matrix influence on epithelial glandular organization. In "seeder" cells, β1 integrin is targeted and localizes to the plasma membrane and is positioned to interact with the basement membrane. During normal cyst development, critical Rac1 activation downstream of β1-integrin signaling is dependent on ARF6 and is required for laminin deposition at the cortex and cell–matrix interactions in developing cysts with positive feedback on Rac1 activation. When ARF6 is depleted, β1-integrin signaling is preempted, Rac1 is not activated above baseline, and cysts do not associate with the basement membrane. As such, cysts are devoid of matrix-derived cues, leading to glandular inversion.

metastatic disease through the lymphatic system (Adams *et al.*, 2004). The acquisition of inverted-cyst phenotypes in basement membrane described above models glandular alterations in the primary niche, whereas the PSC microenvironment better models the lodging and development of a metastasis at collagenous secondary sites. These studies enhance current understanding of the molecular basis of epithelial gland inversion reminiscent of disease states and also highlight the importance of the ECM in dictating glandular phenotype and function.

MATERIALS AND METHODS

Generation of an inducible MDCK^{ARF6si} cell line

The siRNA construct against the coding region of ARF6 has been previously described (Schweitzer and D'Souza-Schorey, 2005). For creation of the MDCK^{ARF6si} cell line, MDCK cells were first stably transfected with the Tet-Repressor element using the T-REx System (Invitrogen, Carlsbad, CA). Tet-Repressive MDCK cells were then transfected with ARF6 siRNA-pcDNA4/TO expression plasmid via Lipofectamine 2000 (Invitrogen). Stable cell lines were subcloned, and depletion of ARF6 in resistant clones was assessed by immunoblotting analysis.

Cell culture and cyst growth assays

Parental MDCK and MDCK^{ARF6si} cells were maintained in DMEM supplemented with 10% tetracycline-free fetal bovine serum, penicillin, and streptomycin. The inducible cell line was switched to media containing 3 μg/ml doxycycline to induce expression of the ARF6 siRNA hairpin.

Cysts were cultured in Matrigel, as described previously (Debnath *et al.*, 2003; O'Brien *et al.*, 2006). Media on cyst cultures was refreshed every 48 h until mature cysts were formed.

For growth of cysts in PSC matrix, single cells were suspended into a neutralized collagen solution, added to eight-well Lab-Tek chamber slides, and allowed to polymerize before DMEM was overlaid on the matrix. Approximately 8000 cells were suspended in 1 ml of collagen. Cysts were cultured as described above.

For activation of Rac1, cells were serum-starved for 6 h prior to addition of 0.25 U/ml of EGF (commercially available as CN02; Cytoskeleton, Denver, CO), to the culture medium. EGF is standardized in CN02 by measurement in units; 100 ng of EGF is 1 unit of CN02. For inhibition of ROCK, 10 μM of Y27632 (Sigma-Aldrich, St. Louis, MO) was added to the culture medium at seeding.

Antibodies and reagents

Primary antibodies used in these studies were mouse anti-GM130 (BD Pharmaceuticals, Franklin Lakes, NJ), rat anti–β1 integrin (Developmental Studies Hybridoma Bank, University of Iowa, Iowa City, IA), rabbit anti–laminin-332 (Abcam, Cambridge, MA), and rabbit anti–laminin-111 (Sigma-Aldrich). The mouse anti–E-cadherin was generously provided by Warren Gallin (University of Alberta) and the mouse anti-gp135 was a kind gift from George Ojakain (SUNY Downstate Medical Center). Secondary antibodies were anti-mouse fluorescein isothiocyanate (FITC), anti-rat FITC, and anti-rabbit FITC (Molecular Probes, Carlsbad, CA). Nuclei were stained using Draq5 (Alexis Biochemicals, San Diego, CA) or ToPro3 (Molecular Probes), and actin filaments were stained with rhodamine-conjugated phalloidin (Molecular Probes). Matrigel was obtained from BD Biosciences (Franklin Lakes, NJ).

PSC was prepared as described previously (Kreger *et al.*, 2010). Briefly, type I oligomeric collagen was acid-solubilized and purified from porcine skin. Lyophilized PSC was dissolved in 0.01 N HCl and was sterilized for cell culture with an overnight exposure to chloroform at 4°C.

Lentiviral and retroviral infection of cysts

A short hairpin RNA against nucleotides 76–98 of the ARF6 coding region was subcloned into the lentiviral expression plasmid pLKO.1 (RNAi Consortium). Lentiviral particles were generated according to the manufacturer's protocol. Virus particles were added to three-dimensional cultures at the single-cell stage. Lentiviral infection caused a moderate repression of ARF6 expression in MDCK cysts (Figure S1).

The retroviral expression plasmids were constructed by subcloning cDNAs encoding an ARF6 transcript that is resistant to the target siRNA (Schweitzer *et al.*, 2009) or Rac1(G12V) into the expression vector pLZRS-IRES-eGFP. Retroviral particles were generated as described previously (Palacios *et al.*, 2001), and cysts were infected at the single-cell stage.

Immunofluorescence microscopy

Three-dimensional cultures were prepared for immunofluorescence microscopy, as previously described (Tushir *et al.*, 2010). Briefly, cyst cultures maintained in eight-well LabTek chamber slides were fixed in 4% paraformaldehyde; this was followed by incubation with primary antibody for 4–5 h, washing, and incubation with fluorophore-conjugated secondary antibodies for 2 h. Chambers were removed from the microscope slide and mounted according the manufacturer's protocol. Slides were viewed using a Bio-Rad MRC 1024 confocal microscope (Hercules, CA). For each experimental condition, more than 50 cysts were visualized.

For direct immunofluorescence microscopy in PSC matrix, three-dimensional cell cultures were fixed in 4% paraformaldehyde; this was followed by staining with rhodamine-phalloidin for visualization of actin filaments. Images of PSC cultures were captured via confocal reflection microscopy performed on an Olympus (Center Vally, PA) Flouview FV1000 confocal system adapted to an Olympus IX81 inverted microscope under a 60× lens or on a Nikon (Melville, NY) A1R-MP Laser Scanning Confocal Microscope. Fibrillar collagen was visualized when samples were illuminated with 488-nm laser light. For indirect immunofluorescence, three-dimensional PSC cultures were treated with collagenase (100U/ml phosphate-buffered saline) for 10–12 min at 37°C. Cysts were fixed with 4% paraformaldehyde, permeabilized, and processed for visualization, as described above.

Rac1-GTP/Rho-GTP pull-down assays

Cyst lysates were isolated from Matrigel, as previously described (Tushir and D'Souza-Schorey, 2007; Tushir *et al.*, 2010), and cell lysates from collagen I cultures were prepared as described in Yu *et al.* (2008). Rac1-GTP levels were measured using p21 activated kinase (PAK) pull-down assay, as previously described (Tushir and D'Souza-Schorey, 2007), and Rho-GTP levels were monitored using the Rhotekin pull-down assay (Cytoskeleton) according to the manufacturer's instructions. Total cell levels of Rac1, Rho A, and tubulin were determined from Western blotting of whole-cell lysate.

ACKNOWLEDGMENTS

We thank James Clancy for helpful discussion. C.L.M. is the recipient of a Chemistry–Biology–Biochemistry Interface graduate training fellowship, supported by T32GM075762. This work was supported in part by RO1CA115316 and funds from the University of Notre Dame to C.D.-S.

REFERENCES

Adams SA, Sherwood AJ, Smith ME (2002). Malignant mesothelioma: PAS-diastase positivity and inversion of polarity in intravascular tumour. Histopathology 41, 260–262.

Adams SA, Smith ME, Cowley GP, Carr LA (2004). Reversal of glandular polarity in the lymphovascular compartment of breast cancer. J Clin Pathol 57, 1114–1117.

Bissell MJ, Rizki A, Mian IS (2003). Tissue architecture: the ultimate regulator of breast epithelial function. Curr Opin Cell Biol 15, 753–762.

Bryant DM, Mostov KE (2008). From cells to organs: building polarized tissue. Nat Rev Mol Cell Biol 9, 887–901.

Debnath J, Brugge JS (2005). Modelling glandular epithelial cancers in three-dimensional cultures. Nat Rev Cancer 5, 675–688.

Debnath J, Muthuswamy SK, Brugge JS (2003). Morphogenesis and oncogenesis of MCF-10A mammary epithelial acini grown in three-dimensional basement membrane cultures. Methods 30, 256–268.

Hebner C, Weaver VM, Debnath J (2008). Modeling morphogenesis and oncogenesis in three-dimensional breast epithelial cultures. Annu Rev Pathol 3, 313–339.

Jiang ST, Chiang HC, Cheng MH, Yang TP, Chuang WJ, Tang MJ (1999). Role of fibronectin deposition in cystogenesis of Madin-Darby canine kidney cells. Kidney Int 56, 92–103.

Kreger ST, Bell BJ, Bailey J, Stites E, Kuske J, Waisner B, Voytik-Harbin SL (2010). Polymerization and matrix physical properties as important design considerations for soluble collagen formulations. Biopolymers 93, 690–707.

Levental KR *et al*. (2009). Matrix crosslinking forces tumor progression by enhancing integrin signaling. Cell 139, 891–906.

Martin-Belmonte F, Mostov K (2008). Regulation of cell polarity during epithelial morphogenesis. Curr Opin Cell Biol 20, 227–234.

Molitoris BA, Nelson WJ (1990). Alterations in the establishment and maintenance of epithelial cell polarity as a basis for disease processes. J Clin Invest 85, 3–9.

Muralidharan-Chari V, Hoover H, Clancy J, Schweitzer J, Suckow MA, Schroeder V, Castellino FJ, Schorey JS, D'Souza-Schorey C (2009). ADP-ribosylation factor 6 regulates tumorigenic and invasive properties in vivo. Cancer Res 69, 2201–2209.

Nassar H, Pansare V, Zhang H, Che M, Sakr W, Ali-Fehmi R, Grignon D, Sarkar F, Cheng J, Adsay V (2004). Pathogenesis of invasive micropapillary carcinoma: role of MUC1 glycoprotein. Mod Pathol 17, 1045–1050.

Nelson WJ (2003). Adaptation of core mechanisms to generate cell polarity. Nature 422, 766–774.

O'Brien LE, Jou TS, Pollack AL, Zhang Q, Hansen SH, Yurchenco P, Mostov KE (2001). Rac1 orientates epithelial apical polarity through effects on basolateral laminin assembly. Nat Cell Biol 3, 831–838.

O'Brien LE, Yu W, Tang K, Jou TS, Zegers MM, Mostov KE (2006). Morphological and biochemical analysis of Rac1 in three-dimensional epithelial cell cultures. Methods Enzymol 406, 676–691.

O'Brien LE, Zegers MM, Mostov KE (2002). Opinion: building epithelial architecture: insights from three-dimensional culture models. Nat Rev Mol Cell Biol 3, 531–537.

Palacios F, D'Souza-Schorey C (2003). Modulation of Rac1 and ARF6 activation during epithelial cell scattering. J Biol Chem 278, 17395–17400.

Palacios F, Price L, Schweitzer J, Collard JG, D'Souza-Schorey C (2001). An essential role for ARF6-regulated membrane traffic in adherens junction turnover and epithelial cell migration. EMBO J 20, 4973–4986.

Paszek MJ *et al*. (2005). Tensional homeostasis and the malignant phenotype. Cancer Cell 8, 241–254.

Rodriguez-Boulan E, Salas PJ (1989). External and internal signals for epithelial cell surface polarization. Annu Rev Physiol 51, 741–754.

Santy LC, Casanova JE (2001). Activation of ARF6 by ARNO stimulates epithelial cell migration through downstream activation of both Rac1 and phospholipase D. J Cell Biol 154, 599–610.

Sanz-Moreno V, Gadea G, Ahn J, Paterson H, Marra P, Pinner S, Sahai E, Marshall CJ (2008). Rac activation and inactivation control plasticity of tumor cell movement. Cell 135, 510–523.

Schweitzer JK, D'Souza-Schorey C (2005). A requirement for ARF6 during the completion of cytokinesis. Exp Cell Res 311, 74–83.

Schweitzer JK, Pietrini SD, D'Souza-Schorey C (2009). ARF6-mediated endosome recycling reverses lipid accumulation defects in Niemann-Pick Type C disease. PLoS One 4, e5193.

Tushir JS, Clancy J, Warren A, Wrobel C, Brugge JS, D'Souza-Schorey C (2010). Unregulated ARF6 activation in epithelial cysts generates hyperactive signaling endosomes and disrupts morphogenesis. Mol Biol Cell 21, 2355–2366.

Tushir JS, D'Souza-Schorey C (2007). ARF6-dependent activation of ERK and Rac1 modulates epithelial tubule development. EMBO J 26, 1806–1819.

Wang AZ, Ojakian GK, Nelson WJ (1990). Steps in the morphogenesis of a polarized epithelium. I. Uncoupling the roles of cell-cell and cell-substratum contact in establishing plasma membrane polarity in multicellular epithelial (MDCK) cysts. J Cell Sci 95, 137–151.

Wilson PD, Sherwood AC, Palla K, Du J, Watson R, Norman JT (1991). Reversed polarity of Na^+-K^+-ATPase: mislocation to apical plasma membranes in polycystic kidney disease epithelia. Am J Physiol 260, F420–F430.

Yamada KM, Geiger B (1997). Molecular interactions in cell adhesion complexes. Curr Opin Cell Biol 9, 76–85.

Yu W, Datta A, Leroy P, O'Brien LE, Mak G, Jou TS, Matlin KS, Mostov KE, Zegers MM (2005). β1-integrin orients epithelial polarity via Rac1 and laminin. Mol Biol Cell 16, 433–445.

Yu W, Shewan AM, Brakeman P, Eastburn DJ, Datta A, Bryant DM, Fan QW, Weiss WA, Zegers MM, Mostov KE (2008). Involvement of RhoA, ROCK I and myosin II in inverted orientation of epithelial polarity. EMBO Rep 9, 923–929.